STUDY OF VSI DRIVE MULTIPHASE RELUCTANCE MACHINE REGARDING TORQUE RIPPLE USING 3D FEA

Boubakar FARADJI[1], Aissa AMEUR[2]

This research paper covering a analysis study focus on the electromagnetic torque ripple origin in multiphase synchronous reluctance machine as one major issue how must be enhanced. In progress studies regarding rotor structure have proven the tie-in relation between improving the type of rotor metal, and the electromagnetic torque quality obtained during the use of this machine as traction or propulsion devices. This work presents a comparison between three and five phase synchronous reluctance machine with the same power order. In the first tentative investigation, two various rotor configurations are carefully studied and compared in order to maximize the machine performance and minimize the torque ripple, Bakelite alternating iron rotor and asymmetrical massive iron rotor and also their relationship with stator slots design. A drive structure used synchronous reluctance machine with a three-phase voltage inverter source as power supply. Three conducing modes are compared, the commands are 120, 150, and 180 degrees for three-phase machine. For five phase machine a five-phase inverter is employed for the drive, and five proposed commands 36, 72, 108, and 144 degrees are compared. Based on analysis results the principals enhance factors are carry out for the electromagnetic torque. However, the study is based on the use of a three-dimension final element method.

Keywords: Reluctance Machine- Rotor Design-Sator Slots-Torque ripple-Voltage Source Inverter

1. Introduction

The reluctance synchronous machine (RSM) is an electromagnetic converter, where operational principle is based on the attraction and repulsion between excited ferromagnetic parts, on the same principle of electric current, the current passes into the conductor which has the weakest resistance in an electric circuit, the magnetic flux itself goes into the least reluctant part for an electromagnetic circuit. Due to the windings distribution around stator and the current variation in the circuit including the rotor motion, the magnetic flux passage from the machine stator to the rotor through the air gap, where the last one will be the seat of electromechanical energy conversion and during that an electromagnetic reluctance torque is generated as result. But in this machine the

[1] University Amin Al-Akkal Haj Moussa Akhamok, Tamanresset, Algeria, e-mail: boubakarluck@yahoo.fr
[2] University Amar Télidji of Laghouat, Algeria, e-mail: a.ameur@lagh-univ.dz

main torque presents a higher torque ripple compared to other motors [1-3]; however, it is highly recommended to improve the SRM design to avoid the degradation of performances such as the poor power factor [4] and the high acoustic noises [5]. In several newest scientific works and publications enhance rotor design by applying geometrical asymmetric form as using skewing rotor or flux barriers, or rotor assisted with permanent magnet cheap ferrite [6-8], or even by selected rotor steps. The stator asymmetrical design is proposed too by create an asymmetrical form to stator slots as it is published in [9], the pulsation of the torque can be reduced. In order to improve the performance of electromagnetic torque, a technological solution is proposed in this research paper by a contribution study to three and five phase machine rotor design, the Bakelite alternating iron allude to change the air gap permanence and have less magnetic interaction with the stator slots, in the same time the impact of stator slots type is clarified by the comparison between the torque obtained in case of semi close stator slots and wide open stator slots. The stator windings repartition is included too, by using shortened three pith winding. In the second half the study is extending by using a voltage source inverter (VSI) operates as power supply source to the SRM. In reference [10] the VSI conduction modes applied are three phase six switches are 120°, 180° and 150° to drive induction machine, in this case the reluctance machine is employed. These classic simple commands give the advantage to fast machine charactering beside reducing calculation time when high accuracy modeling approach such three dimensions final elements analysis. Regarding the five-phase machine 36°, 72°, 108° and 144° commands are applied by five phase ten switches VSI [11]. The comparison between different commands modes with objective to obtain a stable multiphase drive system and to improve the quality of electromagnetic torque delivered during machine rotation with smoothed wave form possible.

2. Synchronous Reluctance Machine Circuit Equivalent:

The simplest multiphase reluctance machine has the same stator configuration as three or five phase induction machine , where the windings are distributed identecly and sinusoidally, each one has N_s equivalent turns and R_s resistance. The rotor has a salient symmetrical structure is shown Fig. 1 [12].

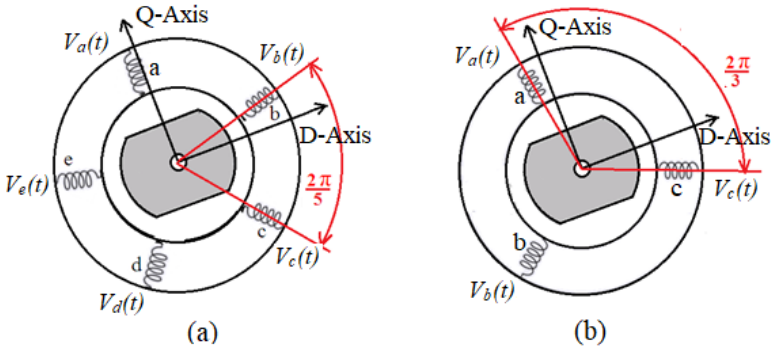

Fig. 1. The SRM structure description for (a) Five phase machine (b) Three phase machine

In order to develop the electrical equivalent circuit for multiphase machine, considered the rotor mechanical position θ is the angle between the rotor D-axis and the stator winding A-axis. The fundamental equation of the stator voltages three and five phase machine can be written as the following equation:

$$\left\{\begin{array}{l}\left.\begin{array}{l}V_a(t)=R_s.i_a(t)+\dfrac{d\Psi_a(\theta,i)}{dt}\\ V_b(t)=R_s.i_b(t)+\dfrac{d\Psi_b(\theta,i)}{dt}\\ V_c(t)=R_s.i_c(t)+\dfrac{d\Psi_c(\theta,i)}{dt}\end{array}\right\}\text{three phase}\\ \left.\begin{array}{l}V_d(t)=R_s.i_d+\dfrac{d\Psi_d(\theta,i)}{dt}\\ V_e(t)=R_s.i_e+\dfrac{d\Psi_e(\theta,i)}{dt}\end{array}\right\}\text{five phase}\end{array}\right. \quad (1)$$

Where $V_{abcde}(t)$, R_s, $i_{abcde}(t)$, Ψ_{abcde} (θ,i) are the stator phases voltages, resistances, currents and total magnetic flux, respectively.

The magnetic flux of multiphase machine is variable and expressed as a function of the angle θ and the stator windings currents. The flux linkages generated from five phase windings can be regrouped and arranged in matrix form "(2)":

$$\begin{bmatrix}\Psi_a(\theta,i)\\ \Psi_b(\theta,i)\\ \Psi_c(\theta,i)\\ \Psi_d(\theta,i)\\ \Psi_e(\theta,i)\end{bmatrix}=\begin{bmatrix}\Psi(\theta,i_a) & \Psi_{ab}(\theta,i_a,i_b) & \Psi_{ac}(\theta,i_a,i_c) & \Psi_{ad}(\theta,i_a,i_d) & \Psi_{ae}(\theta,i_a,i_e)\\ \Psi_{ba}(\theta,i_a,i_b) & \Psi_b(\theta,i_b) & \Psi_{bc}(\theta,i_b,i_c) & \Psi_{bd}(\theta,i_a,i_d) & \Psi_{bd}(\theta,i_a,i_e)\\ \Psi_{ca}(\theta,i_a,i_c) & \Psi_{cb}(\theta,i_c,i_b) & \Psi_{ca}(\theta,i_c) & \Psi_{cd}(\theta,i_d,i_c) & \Psi_{ce}(\theta,i_e,i_c)\\ \Psi_{da}(\theta,i_d,i_a) & \Psi_{db}(\theta,i_d,i_b) & \Psi_{dc}(\theta,i_d,i_c) & \Psi_d(\theta,i_d) & \Psi_{de}(\theta,i_d,i_e)\\ \Psi_{de}(\theta,i_e,i_a) & \Psi_{eb}(\theta,i_e,i_b) & \Psi_{ec}(\theta,i_c,i_e) & \Psi_{ed}(\theta,i_d,i_e) & \Psi_e(\theta,i_e)\end{bmatrix} \quad (2)$$

- If $\frac{d\Psi(\theta,i)}{di}$ is the instantaneous inductance L(θ,i), and $\frac{d(\theta)}{dt}=\omega$ is the angular velocity of rotation is related to the electric pulsation.
- If the courant variation is independent of the rotor position.

The equation "(1)" is developed to give the extended voltages equation "(3)" below with a term corresponding to the derivatives of the currents with respect to time, it is defined by Transformation Electromotive Force (E_t) and a term corresponding to the derivative of the matrix of inductance by compared to time defined by Rotation Electromotive Force (Er).

$$\begin{cases} V_a(t) = R_s.i_a(t) + L_a\dfrac{di_a(t)}{dt} + L_{ab}\dfrac{di_b(t)}{dt} + L_{ac}\dfrac{di_c(t)}{dt} + L_{ad}\dfrac{di_d(t)}{dt} + L_{ae}\dfrac{di_e(t)}{dt} + E_{at} \\ V_b(t) = R_s.i_b(t) + L_b\dfrac{di_b(t)}{dt} + L_{ba}\dfrac{di_a(t)}{dt} + L_{bc}\dfrac{di_c(t)}{dt} + L_{bd}\dfrac{di_d(t)}{dt} + L_{be}\dfrac{di_e(t)}{dt} + E_{bt} \\ V_c(t) = R_s.i_c(t) + L_c\dfrac{di_c(t)}{dt} + L_{cb}\dfrac{di_b(t)}{dt} + L_{ac}\dfrac{di_a(t)}{dt} + L_{cd}\dfrac{di_d(t)}{dt} + L_{ce}\dfrac{di_e(t)}{dt} + E_{ct} \\ V_e(t) = R_s.i_e(t) + L_e\dfrac{di_e(t)}{dt} + L_{ea}\dfrac{di_a(t)}{dt} + L_{eb}\dfrac{di_b(t)}{dt} + L_{ec}\dfrac{di_c(t)}{dt} + L_{ed}\dfrac{di_d(t)}{dt} + E_{et} \\ V_d(t) = R_s.i_d(t) + L_d\dfrac{di_d(t)}{dt} + L_{da}\dfrac{di_a(t)}{dt} + L_{db}\dfrac{di_b(t)}{dt} + L_{dc}\dfrac{di_c(t)}{dt} + L_{de}\dfrac{di_e(t)}{dt} + E_{dt} \end{cases} \quad (3)$$

The electrical equivalent schema for five-phase reluctance machine, according to the equation "(3)" is represented in Fig. 2 below.

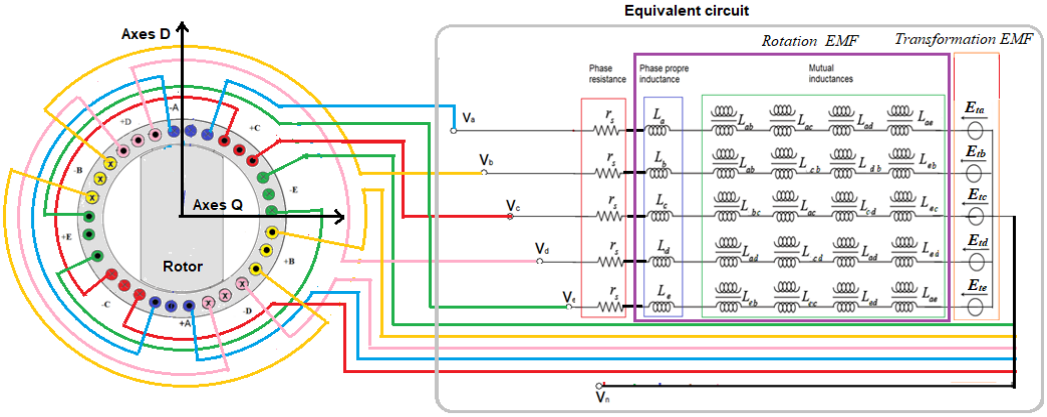

Fig. 2. Five phase reluctance machine equivalent circuit

3. Model analysis with three dimensions FEM:

Reluctance machine electromagnetic model is defined as magnetostatic, obtained by neglecting the time derivatives in Maxwell equations [13]. Thus, given a divergence free stationary source current density J, the magnetic field H and the magnetic induction B satisfy the following equations "(4)":

$$\begin{cases} \overrightarrow{rot}\,\vec{H} = \vec{J} \\ \vec{B} = \overrightarrow{rot}\vec{A} \end{cases} \begin{cases} div\,\vec{J} = 0 \\ div\,\vec{B} = 0 \\ div\,\vec{A} = 0 \end{cases} \quad (4)$$

The model formulation is given by terms of scalar potentials vector "(5)" in three dimensions in cylindrical coordinates:

$$\begin{cases} \text{rot}\,(\text{rot}\,A) = \mu J \\ \frac{1}{r}\frac{\partial}{\partial r}\left(r\frac{\partial A}{\partial r}\right) + \frac{1}{r^2}\frac{\partial^2 A}{\partial \varphi^2} + \frac{\partial^2 A}{\partial Z^2} = \mu J \end{cases} \quad (5)$$

Where:

μ: Metal magnetic permeability, $\vec{A}$: Magnetic vector potential, $\vec{j}$: Current density vector.

The FEM is applied to resolve this magnetostatic problem in three steps. First draw the machine geometry design in FLUX 3D environment *Table.1* gives machine geometry parameters for all simulation case. Both machine parts metals specifications are insured, the machine rotor is made of a single asymmetrical piece of ferromagnetic metal [15] (Non-Oriented Grain Silicon-Iron) in first case than it is substituted by assembling structure frame nonmagnetic (Bakelite) and ferromagnetic metals in second case. Then geometry mesh consists of tetrahedral finite elements. Typical number of equations is about 52571 nodes for Iron Asymmetric rotor and 97391 nodes for Bakelite alternating rotor . Non meshed coils are used to represent the machine widings repartition and that gives the adventege to reduce FEM three dimunsions acurancy calulate time. After that results exploitation is presented [14]. Fig.3 illustrates all steps munched before for three and five-phase reluctance machine obtained in FLUX 3D environment.

Table 1.

Machines Geometry Parameters

Geometry Parameter	Three Phase machine open wide slot (mm)	Three Phase machine semi close slot (mm)	Five Phase machine (mm)
The stator			
Number of stator slots	24	24	30
Stator outer diameter	160	160	160
Stator inner diameter	92.7	92.7	92.7
Axial length	100	100	100
Number of slots in phase and pole	4	4	3
The rotor			
Air gap E	0.8	0.8	0.8
Rotor outer diameter	91.9	91.9	91.9
The Stator slot			
Stator slot opening angle λ	0°	45°	45°
Stator slot height C	16.8	16.8	16.8
Min width of stator slot A	6.7	6.7	6.7
Max width of stator slot B	6.7	4.5	4.5

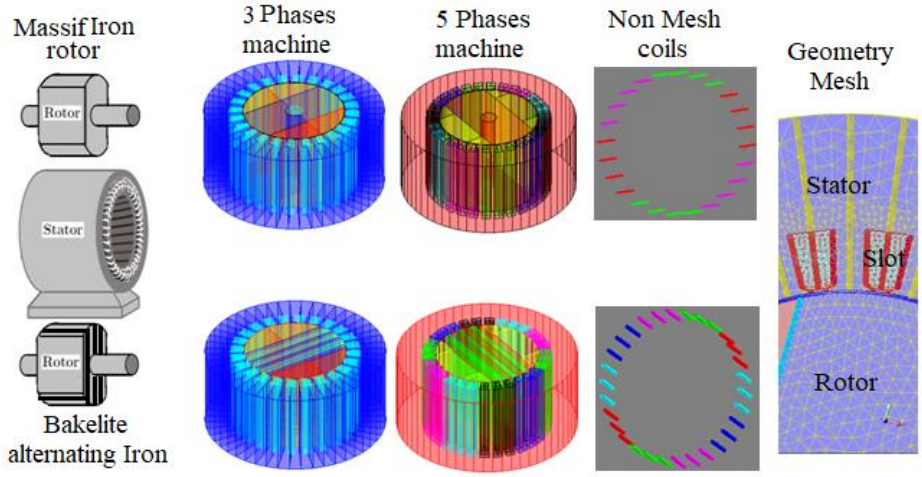

Fig. 3. The Iron and Bakelite alternating rotor designs, then three and five phase machine geometry obtained in FLUX3D, after that the non-meshed coil used in case of three and five phase machine, and at last zoom on the mesh used for the machine

3.1 stator slots effect analyze:

To evaluate the stator slots designs effects on electromagnetic torque characteristics ,two different slot design are used for machine stator Fig.4. The slots parametars A,B,C are described in *Table.1*.

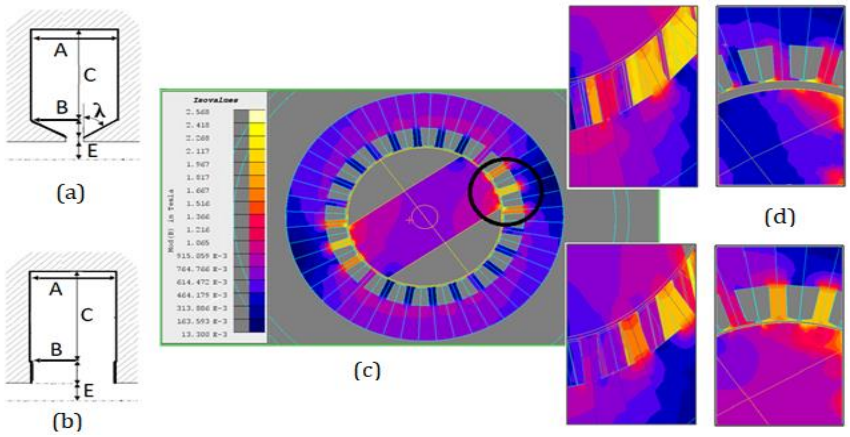

Fig. 4. (a) The semi close stator slots, (b) The wide-open stator slots (c) Three phase machine magnetic flux density distribution, (d) The semi close and wide open stator slots magnetic flux density distribution at the maximal and the minimal positions

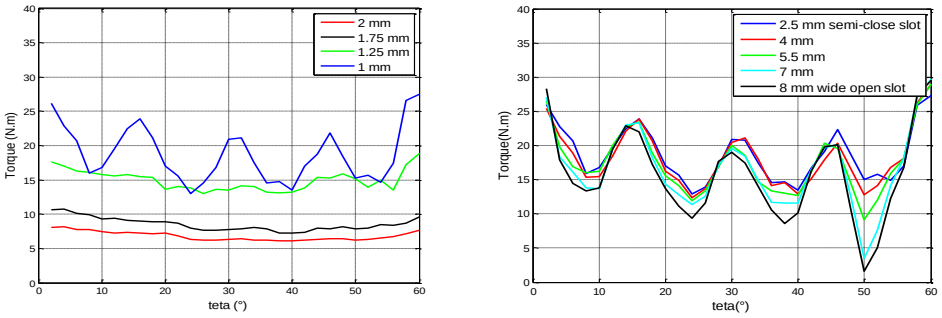

(a) (b)

Fig. 5. (a) The electromagnetic torque variation with machine airgap E changing (b) The electromagnetic torque variation with stator slots opening B changing

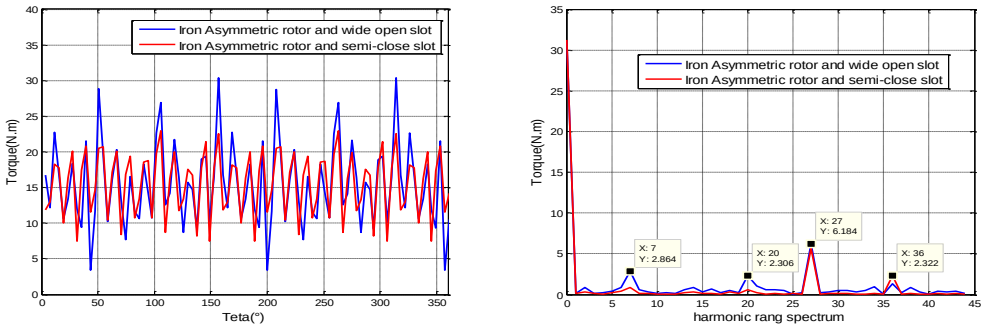

(a) (b)

Fig. 6. (a) The electromagnetic torque variation for semi close stator slots and wide open stator slots, (b) The electromagnetic torque FFT

In first case the stator is occupied with semi close slots, the aregap E is increase in every step with 0.25 mm, the electomagnetec torque is illestrated in Fig. 5(a). As it can be seen the maximum and average level of the torque increase as a function of airgap width, however, at the same time the torque ripple also increases. In the second time the stator is occupied with semi close slotes B passing to wide open slots with 2.5 mm step evry time, the electromagnetic torque variation is represented in the Fig. 5(b).

Fig.6(a) shows a comparison between the electromagnetic torque variation with semi close stator slots for lowest larger 2,5mm and largest wide open stator slots 8mm, the FFT in Fig.6(b) cofirme that with semi close slots the harmonics 7 and 21 are sineficantly redused , and that inhance the torque in case of semi close slots.

3.2 Rotor design effect analyzes with three phase machine:

The Iron rotor can be replaced by Bakelite alternating rotor, the Fig.7 (a) and Fig.7 (b) shows a comparison between stator occupied by wide open slots and semi close slots electromagnetic torque produced.

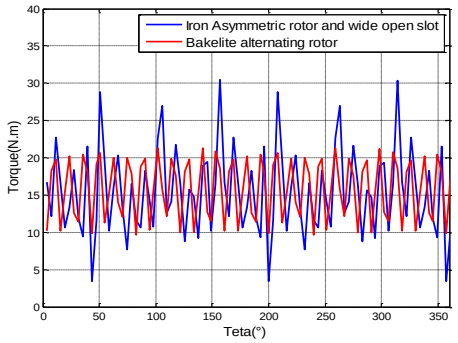

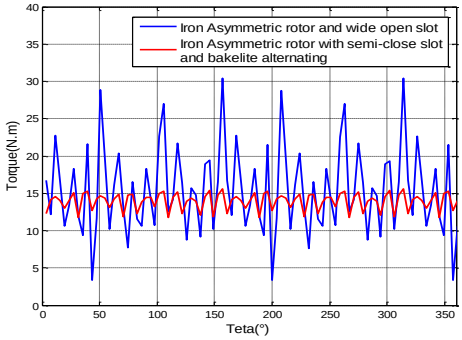

(a) (b)

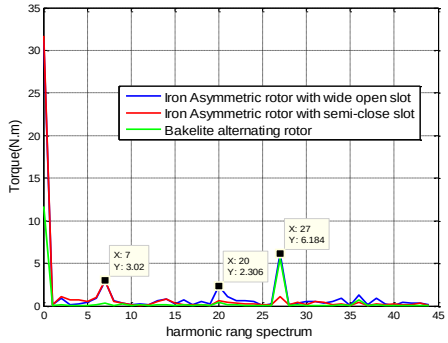

(c)

Fig. 7. (a) The electromagnetic torque variation with wide open stator slots and Bakelite alternating rotor (b) The electromagnetic torque variation with wide open stator slots and Bakelite alternating rotor (c) The electromagnetic torque FFT

The Iron rotor presents the highest torque ripple in electromagnetic torque instantaneous evolution, and it is confirmed that the employment of Bakelite alternating rotor reject the harmonic order from harmonic 20 to 27 and eliminate the harmonic 7. The use of semi close slots and Bakelite alternating rotor in the same time allowed to reduced torque ripple (peak) from 30 N.m. to 20 N.m. with minimal reduction in torque rating around average torque of 15 N.m .

3.3 Rotor design effect analyzes with five phase machine:

In this part five phase reluctance machine massif rotor is substitute by Bakelite alternating rotor, and a comparison for the electromagnetic torque is illustrated in Fig. 9. The Fig. 8(a), (c) shows the magnetic flux density and lines distribution in both cases, two magnetic poles appear in the machine. In case of Bakelite alternating rotor, the flux lines are more concentrated around iron rotor and that create the same thing in stator flux lines Fig. 8(b), (d).

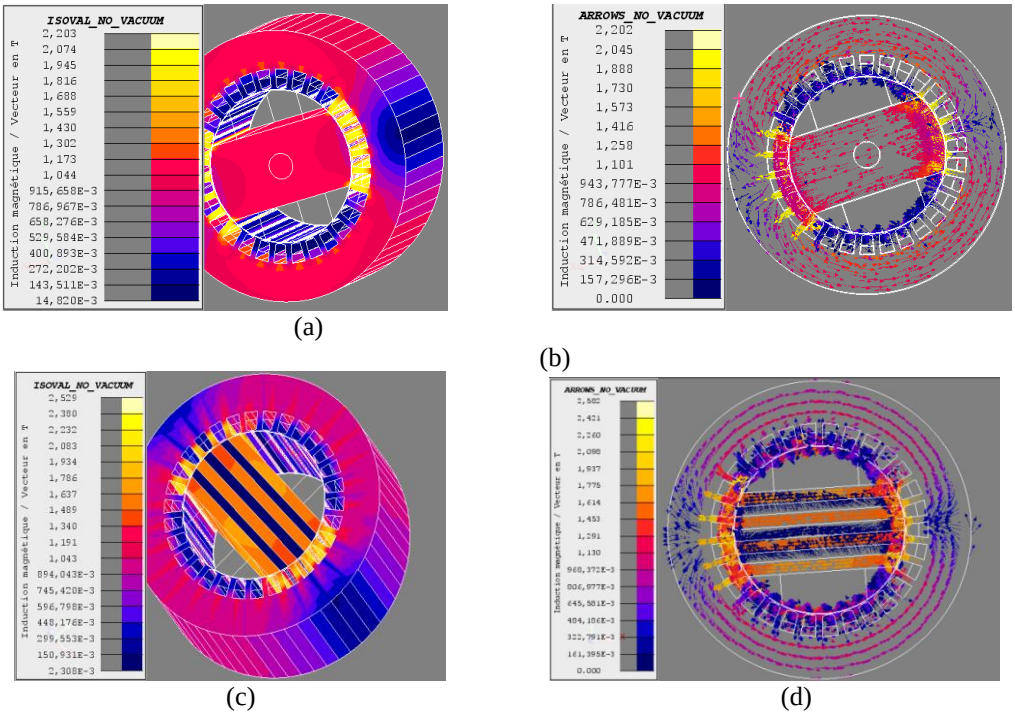

Fig. 8. The Five phase SRM massive rotor (a) Magnetic flux density (b) Magnetic flux lines, The Five phase SRM Bakelite alternating rotor (c) Magnetic flux density (d) Magnetic flux lines

The five-phase machine electromagnetic torque is dedicated in Fig. 9 (a), the wave form presents less ripple than three phase machine even with Bakelite alternating rotor. The five-phase machine occupied by Bakelite alternating rotor produce the lowest torque ripple. Moreover, the FFT harmonic components in Fig.

9(b), show that harmonic component is rejected to 30, because of the stator slots number.

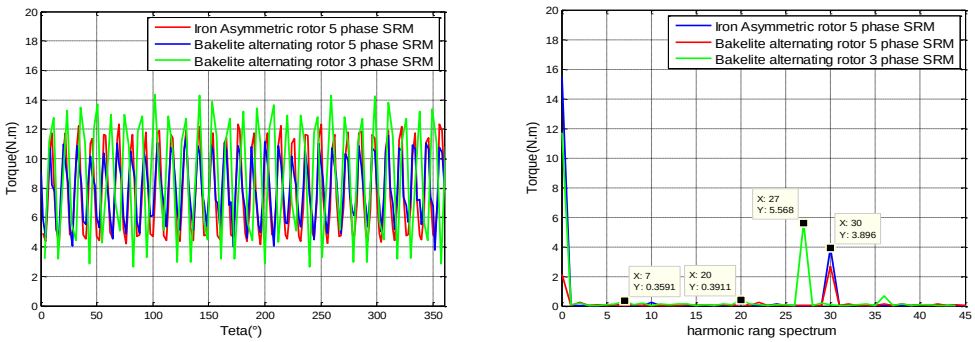

(a) (b)

Fig. 9. (a) The Five phase SRM massive rotor and Bakelite alternating rotor electromagnetic torque variation (b) The electromagnetic torque FFT

4. Association of synchronous reluctance machine to VSI converter:

A detailed open loop of three and five phase drive structure is elaborated in Figure10 (a),(b) respectively . The DC link voltage is not adjusted as the diodes operate in natural conduction angles from with full power rectified. Large capacitor is connected at the input terminal to make the DC input constant and also suppress the harmonics fed back to the source.

The capacitor capacity value can be estimated and calculated from the formula" (6) ":

$$C_{min} = \frac{2 \times P}{(U_{max}^2 - U_{min}^2) \times f_{rectifier}} \quad (6)$$

Where P: Power in load, $f_{rectifier}$: Rectifier output frequency , U_{max}: Maximal voltage value in the out of rectified voltage , U_{min} : Minimal voltage value in the out of rectified voltage .

The frequency of the fundamental output is controlled from the fully controllable semiconductor (switch) based voltage source inverter (VSI) . The inverter is operating in the quasi-square wave mode.

A six steps bridge is used for three phase inverter by using six switches, two switches for each phase in case of three phase drive system. Each step is defined as a change in the time operation for each switch to the next switch in proper sequence. For one cycle 360°, each step would be of 60° interval for a six step inverter [16]. Thus, overall control schema is represented in Fig. 11(a) three phase drive system diagrams for, 120°,150°, and 180° conducing mode are compared.

The five-phase drive structure with five phase VSI, is shown in Fig. 10(b). The inverter outputs are noted with lower case letters (a,b,c,d,e) [17]. Two switches for each phase, in this case each step is defined as a change in the time operation for each switch to the next switch in proper sequence. For one cycle 360º, each step would be of 36º interval, then the conducing mode it is shifted to 72º interval, than to 108º, than to144º as it is represented in the diagram Fig.11(b).

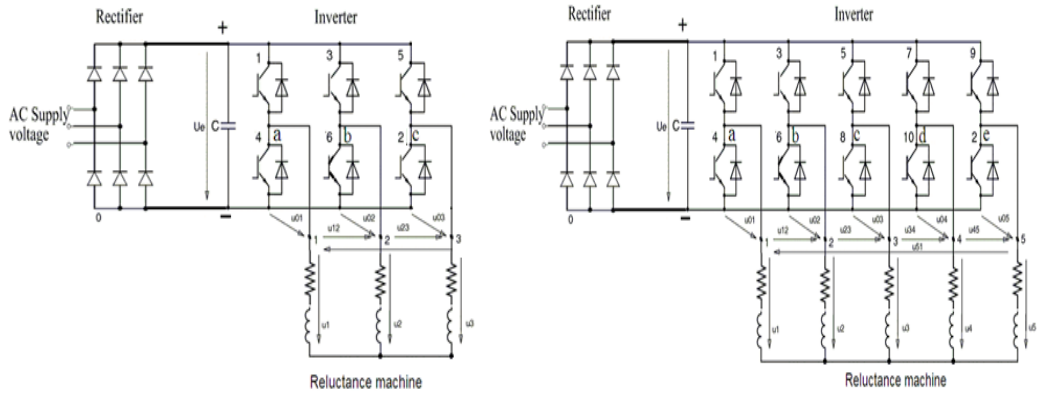

(a) (b)

Fig. 10. (a) Three phase drive structure with three phase VSI power circuit (b) Five phase drive structure with five phase VSI power circuit

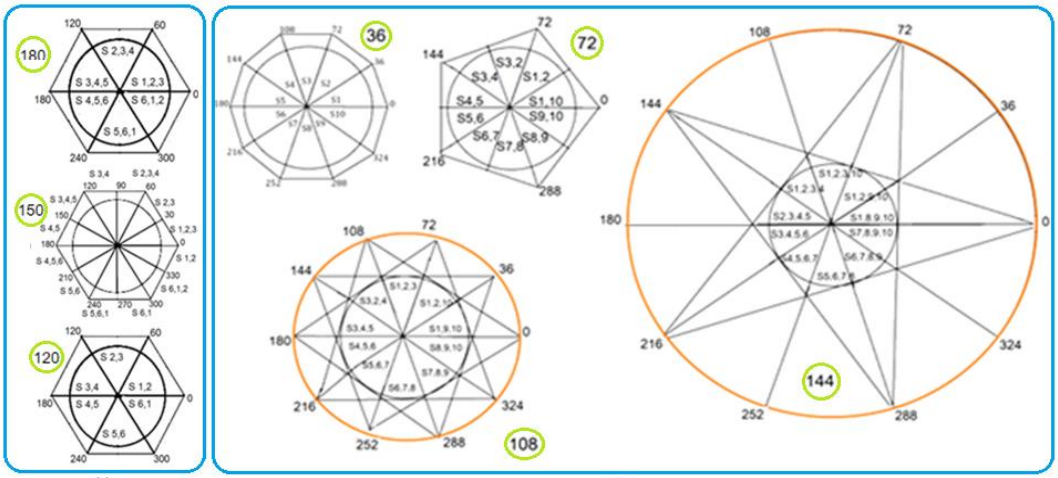

(a) (b)

Fig. 11. (a) The three conducing mode 120°,150°, and 180° one cycle diagram (c) The five conducing mode 36°,72°,108°and 144° one cycle diagram

The Fig.12 (a) show first phase current waveforms in 120°,150°, and 180° conducing modes, the current presents harmonics the maximal variation value is obtained by 120° than fluctuation is reduced for 180° and 150° conducing modes. The Fig.12 (b) show current waveforms for five phase machine, the current waveform present an interval where it is totally turned off and others with picks in

36° and 72° modes. For 108° and 144° conducing modes the current increase and present very high maximal value.

The magnetic flux variation for the three conducing mode 120°,150°, and 180° is represented in Fig.13(a) , and it variation is all most sinusoidal form. The Fig.13(b)shows the magnetic flux variation for the five phase conducing modes 36°,72°,108°and 144°, comparing to three phase modes the maximal value is reduced and the waveform present fluctuations.

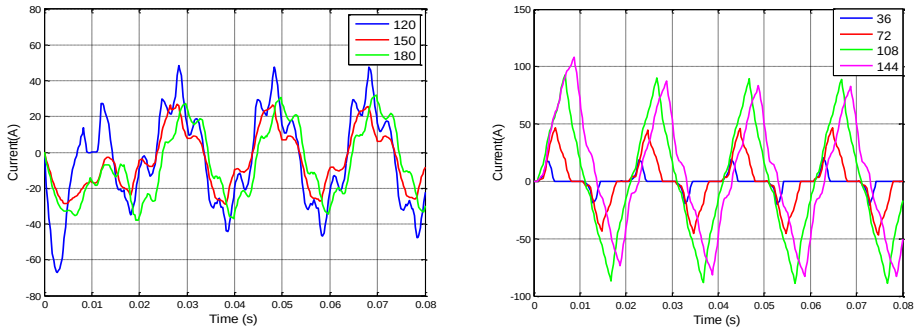

(a) (b)

Fig. 12. (a) The current variation for three conducing mode 120°,150°, and 180° (b) The current variation for three conducing mode 36°,72°,108°and 144°

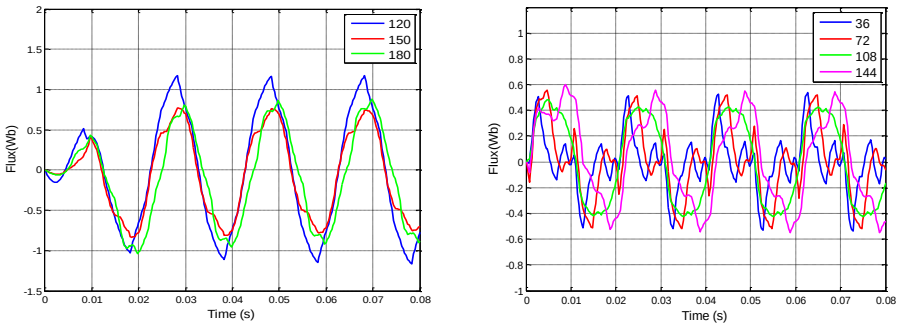

(a) (b)

Fig. 13. (a) The magnetic flux variation for the three conducing mode 120°,150°, and 180° (b) The magnetic flux variation for the five conducing mode 36°,72°,108°and 144°

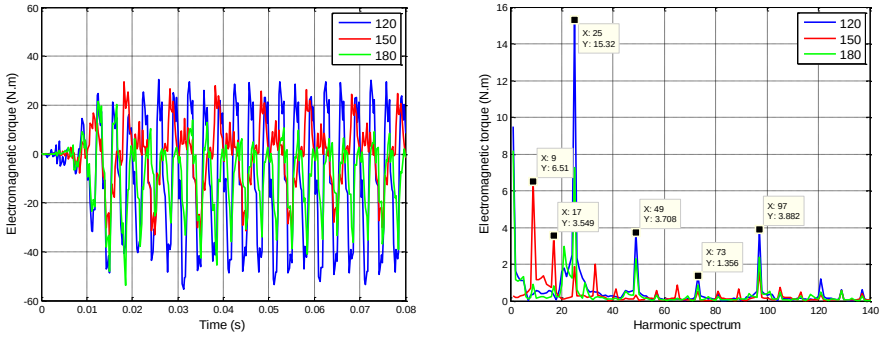

(a) (b)

Fig. 14. (a) The electromagnetic torque variation for three conducing mode 120°,150°, and 180° (b) The electromagnetic torque FFT for the three conducing mode 120°,150°, and 180°

The electromagnetic torque obtained by 120 ^{o},150^{o}, and 180^{o} conducing modes is illustrated in Fig. 14 (a), it can be observed that electromagnetic torque with less ripple is with 150^{o} than 180^{o}. By comparing the current variation in Fig.12 (a), the torque peak value will be reduced significantly due to the current harmonic reducing. The reluctance torque ripple has decreased from 43% with the 120^{o} to 30% with 150^{o}, approximately.

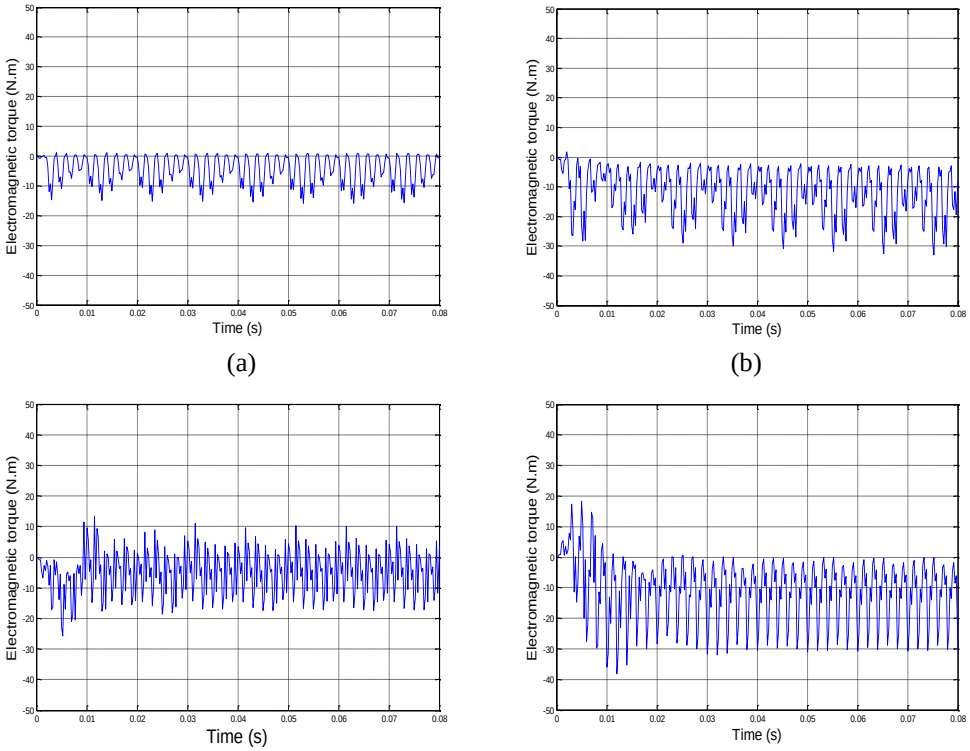

(a) (b)

(c) (d)

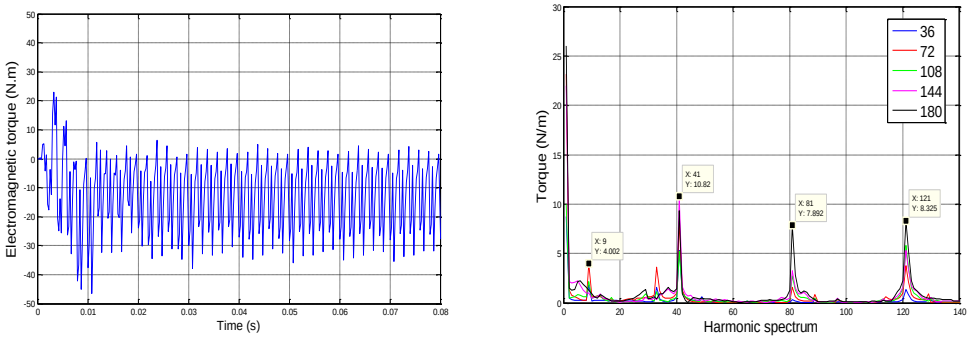

(e) (f)

Fig.15.The electromagnetic torque variation for three conducing mode (a)36°,(b)72°,(c)108°, (d)144°,(e)180° (f) The electromagnetic torque FFT for the five conducing mode 36°,72°,108°,144° and 180°

The electromagnetic torque obtained for each conducing mode shows in Fig. 15 and it can be observed that electromagnetic torque with less ripple is with 36° the comparison of torque FFTs in Fig 15(f), the 9, 41 and 81 harmonics are weaker in case of 36° conducing mode and provide a fickler behavior on the torque and the torque ripple peak value had significantly reduced, but the massive torque is lower in this case.

5. Conclusions

This paper contributes to enrich the discussion and to verify the feasibility of using multiphase reluctance machine as alternative to Inverter driven.

Hence study first result is that the transient electromagnetic torque and torque ripple for five phase machine are low whereas they are high for three phase machine. It can be concluded too that the reluctance torque ripple is the main component of the total generated torque cannot totally eliminated but reduced only.

The second results, machine rotor and stator slots design influences on torque ripple are presented with high advantage offered by using Bakelite Alternating rotor and semi close stator slots to reduce the electromagnetic torque ripple. The machine design study can be extended to investigate asymmetrical stator slots, and also asymmetrical windings such as fractional windings technique, more over that rotor geometry design can improved too.

In the study second section, since the machine technical control type is adopted to offer the best robustness possible, the quasi square wave mode under several switching conducing modes proposals gives a general idea about system fast responses and for more flexibility and robustness the AC/DC part can be

substituted by another electronic converter which operate on specific voltage and load conditions, with more power exchanging and electromagnetic torque control.

Finally, experimental validation is required on laboratory prototype machine and that for best design realization with control implementation to the drive system.

R E F E R E N C E S

[1]. M. Tursini, M. Villani, G. Fabri, A. Credo, F. Parasilit, A. Abdelli " Synchronous Reluctance Motor: Design, Optimization and Validation" SPEEDAM Conference ,Amalfi Coast Italy 20-22 June 2018

[2]. A. E. Nik1 , J. Faiz1"Optimization of Synchronous Reluctance Motor Based on Radial Basis Network" Serbian Journal Of Electrical Engineering vol. 17, No. 2, pp. 223-234 ,June 2020

[3]. Q. Chen, Y. Tang, E. A. Lomonova " Torque optimization of Synchronous Reluctance Motor for Electric Powertrain Application" EVER Conference,Monte-Carlo Monaco, 8-10 May 2019

[4]. L. N. Langue, G. Friedrich, S. Vivier, K. El K. Benkara" Optimization of synchronous reluctance machines for high power factor" ICEM Conference, Lausanne Switzerland, 4-7 September 2016

[5]. X. Liu, Y. Li, Z. Liu, T. Ling , Z Luo" Analysis and design of a high power density permanent magnet-assisted synchronous reluctance machine with low-cost ferrite magnets for EVs/HEVs" The international journal for computation and mathematics in electrical and electronic engineering, vol. 35 N°. 6, pp. 1937-1948,November 2016

[6]. A. Arafat . Md. Z. Islam Md T. Bin Tarek, S. Choi "Transient Stability Comparison between Five-phase and Three-phase Permanent Magnet Assisted Synchronous Reluctance Motor" ITEC Conference, Long Beach CA USA,13-15 June 2018

[7]. Md. Islam ,S. Choi" Performance comparison between three-phase and five-phase ferrite permanent magnet assisted synchronous reluctance motor" ITEC Conference, Navy Pier in Chicago IL ,22-24 June 2017

[8]. S. S. R. Bonthu1, S. Choi1, J. Baek "Comparisons of three-phase and five-phase permanent magnet assisted synchronous reluctance motors" IET Electr. Power Appl., vol.10, N°.5, pp. 347-355 ,May 2016

[9]. M. Xu, G. Liu, W. Zhao, N. Aamir" Minimization of torque ripple in ferrite-assisted synchronous reluctance motors by using asymmetric stator" AIP Advances vol.8, N°.5 , pp. 056606-1 – 056606-5 , 2018

[10]. M. P. Abhishek "THD Comparison for 180, 120 & 150 Degree Conduction Mode of Three Phase Inverter" Journal IJSRD vol. 6, N°. 03, pp.145-149, 2018

[11]. M. Bermúdez ,C. Martín ,I.G.Prieto ,M. J. Durán ,M. R. Arahal ," Predictive current control in electrical drives: an illustrated review with case examples using a five-phase induction motor drive with distributed windings" IET Electr. Power Appl., vol. 14 N°. 8 pp. 1291-1310, 2020

[12]. Y. Hua, H. Zhu, M. Gao, Z. Ji "Design and Analysis of Two Permanent-Magnet-Assisted Bearingless Synchronous Reluctance Motors with Different Rotor Structure" Journal Energies ,Vol 14,N°. 879, pp.1-17,2021

[13]. I. Mahariq , a. Erciyas " A spectral element method for the solution of magnetostatic fields" Turk J Elec Eng & Comp Sci vol. 25,N°.4, pp.2922 – 2932 , 2017

[14]. FLUX3D – Altair Flux™ User Guide ,vol.1, 2019

[15]. R. A. Botelhoa, S. B. Diniza , M. A. da Cunhab , L. P. Brandaoa" Properties of NGO 3% Silicon Steel Asymmetrically Cold Rolled" Materials Research. vol .18,N°. 2, pp.143-147. 2015

[16]. R. Shah, D. Shah, P. Shah , S. Thakur"Simulation and Analysis of 150° Conduction Mode For Three Phase Voltage Source Inverter" International Journal IJERD vol.8, N°.9, pp. 05-10, April 2016

[17]. S. Moinoddin, A. Iqbal, E. M. Elsherif" Five-phase induction motor drive for weak and remote grid system" International Journal of Engineering, Science and Technology vol. 2, No. 2, pp. 136-154,2010